

ORIGINAL ARTICLE

Platelet-targeting sensor reveals thrombin gradients within blood clots forming in microfluidic assays and in mouse

J. D. WELSH,* † T. V. COLACE,* R. W. MUTHARD,* T. J. STALKER‡, L. F. BRASS‡ and S. L. DIAMOND*

*Institute for Medicine and Engineering, Department of Chemical and Biomolecular Engineering; †Department of Biochemistry and Molecular Biophysics; and ‡Department of Medicine, University of Pennsylvania, Philadelphia, PA, USA

To cite this article: Welsh JD, Colace TV, Muthard RW, Stalker TJ, Brass LF, Diamond SL. Platelet-targeting sensor reveals thrombin gradients within blood clots forming in microfluidic assays and in mouse. *J Thromb Haemost* 2012; 10: 2344–53.

Summary. *Background:* Thrombin undergoes convective and diffusive transport, making it difficult to visualize during thrombosis. We developed the first sensor capable of revealing inner clot thrombin dynamics. *Methods and results:* An N-terminal-azido thrombin-sensitive fluorescent peptide (ThS-P) with a thrombin-releasable quencher was linked to anti-CD41 using click chemistry to generate a thrombin-sensitive platelet binding sensor (ThS-Ab). Rapid thrombin cleavage of ThS-P ($K_m = 40.3 \mu\text{M}$, $k_{\text{cat}} = 1.5 \text{ s}^{-1}$) allowed thrombin monitoring by ThS-P or ThS-Ab in blood treated with 2–25 μM tissue factor (TF). Individual platelets had > 20-fold more ThS-Ab fluorescence after clotting. In a microfluidic assay of whole blood perfusion over collagen \pm linked TF (wall shear rate = 100 s^{-1}), ThS-Ab fluorescence increased between 90 and 450 s for 0.1–1 molecule-TF μm^{-2} and co-localized with platelets near fibrin. Without TF, neither thrombin nor fibrin was detected on the platelet deposits by 450 s. Using a microfluidic device to control the pressure drop across a thrombus forming on a porous collagen/TF plug (521 s^{-1}), thrombin and fibrin were detected at the thrombus-collagen interface at a zero pressure drop, whereas 80% less thrombin was detected at 3200 Pa in concert with fibrin polymerizing within the collagen. With anti-mouse CD41 ThS-Ab deployed in a mouse laser injury model, the highest levels of thrombin arose between 40 and 160 s nearest the injury site where fibrin co-localized and where the thrombus was most mechanically stable. *Conclusion:* ThS-Ab reveals thrombin locality, which depends on surface TF, flow and intrathrombus pressure gradients.

Keywords: fibrin, permeation, platelet, shear rate, thrombin, tissue factor.

Introduction

During coagulation, membrane-associated prothrombinase (Xa/Va) cleaves prothrombin to release active thrombin, a soluble protease that can cleave protease-activated receptors (PAR1 and PAR4 on human platelets) as well as activate fibrinogen to fibrin monomer. As a soluble species, thrombin is subject to diffusive transport as well as convective transport via intrathrombic permeation (if pressure gradients exist [1,2]) or via blood flow once thrombin leaves the clot [3,4]. Additionally, thrombin can bind platelet GPIb to localize its activity on the platelet surface [5,6] or thrombin can be inhibited by antithrombin or sequestered into polymerizing fibrin. The generation and subsequent transport of activated factor X (FXa) and thrombin from tissue factor (TF)-rich sites of Xa and activated factor (FIXa) formation have an important controlling effect on the rate and extent of thrombus growth through platelet activation and fibrin stabilization [7,8]. Formation of the intrinsic tenase (FIXa/VIIIa), as well as feedback pathways such as thrombin-mediated production of FIXa, may also impact the spatio-temporal concentration profiles of thrombin within a clot [9]. Thrombin activation of platelets induces the release of ADP, thromboxane, as well as pro-inflammatory cytokines and surface display of P-selectin, thus promoting white blood cell recruitment and inflammation [10].

Various techniques currently exist to monitor thrombin in closed systems. These techniques measure endogenous end-products such as thrombin-antithrombin (TAT) or exogenously added reporter substrates [11–15]. Under physiological flow conditions, thrombin detection becomes extremely difficult owing to the convective removal of coagulation products or fluorogenic sensing molecules. Fibrin deposition can be monitored under flow as an important surrogate of thrombin activity. However, fibrin deposition is also subject to convective effects via fibrin monomer dilution and flow modulation of fibrin assembly [16,17]. Also, thrombin can affect platelet deposition at concentrations below that needed to generate fibrin [3,8].

Correspondence: Scott L. Diamond, Institute for Medicine and Engineering, Department of Chemical and Biomolecular Engineering, University of Pennsylvania, Philadelphia, PA 19104, USA.
Tel.: +1 215 573 5702; fax: +1 215 573 7227.
E-mail: sld@seas.upenn.edu

Received 31 May 2012, accepted 31 August 2012

In spite of its central role, thrombin activity has never been visualized *in vivo*. We developed a thrombin sensitive antibody (ThS-Ab) that binds platelet CD41 (α_{IIb}) to ensure its incorporation throughout the growing thrombi. The sensor consisted of a thrombin sensitive peptide (ThS-P) that was linked to an anti-CD41 antibody and was rapidly cleaved by thrombin to provide a fluorescent signal. In this study, we characterized this thrombin sensor to provide novel information about thrombin localization on activated platelets and within clots.

Methods

Materials

Thrombin-sensitive peptide (ThS-P) *azidoacetyl alanine-K(5FAM)GALVPRGSAGK(CPQ2)* was custom synthesized (2143 MW, > 95% purity; CPC scientific, Sunnyvale, CA, USA) and dissolved in DMSO (20 mM ThS-P). The cleavage site VPR|G was chosen based on the strong preference by thrombin for proline in the P2 position [17] and the prior use of boc-Val-Pro-Arg-MCA [10]. The following reagents were stored according to manufacturers' instructions: dibenzylcyclooctyne-NHS ester (DBCO; Click Chemistry Tools, Scottsdale, AZ, USA), mouse monoclonal anti-human CD41 PM6/248 (azide free; AbD Serotec, Raleigh, NC, USA), PE-mouse monoclonal anti-human CD61, Cy-5 Annexin V (BD Pharmingen, San Diego, CA, USA), Cy5-anti human fibrin (Gift from Dr. M. Poncz, Children's Hospital of Pennsylvania), anti-collagen type 1 antibody and PE-mouse monoclonal anti-human CD42b (Ak2; Abcam, Cambridge, MA, USA), anti-mouse CD41 F(ab)2 fragments (clone MWReg30; BD Bioscience, San Jose, CA, USA), anti-mouse fibrin (clone 59D8, gift from Dr. H Weiler, Blood Center of Wisconsin), thrombin, Gly-Pro-Arg-Pro (GPRP), corn trypsin inhibitor (CTI; Haematologic Technologies, Essex Junction, VT, USA), sodium citrate (Sigma-Aldrich, St. Louis, MO, USA), HEPES ((*N*-(2-hydroxyethyl)piperazine-*N'*-2-ethanesulfonic acid; Fisher Scientific, Pittsburg, PA, USA), recombinant tissue factor (Sekisui, Stamford, CT, USA), phosphatidylcholine (PC), phosphatidylserine (PS), and biotinylated phosphoethanolamine (bPE; Avanti Polar Lipids, Alabaster, AL, USA), Streptavidin and Triton X-100 (Sigma-Aldrich), and BioGel P-6 gel (Bio-Rad, Hercules, CA, USA). In accordance with the University of Pennsylvania Internal Review Board, human blood was collected from healthy donors via venipuncture and anticoagulated with CTI (50 $\mu\text{g mL}^{-1}$) or sodium citrate (1:9 by volume) and then recalcified with CaCl_2 (15 mM final concentration).

Thrombin sensitive antibody (ThS-Ab) synthesis

A volume of 10 μL of anti-human CD41 (1 mg mL^{-1} , azide free) was mixed with 5 μL of DBCO-NHS ester (357 μM , 0.7% DMSO by vol. in HEPES-buffered saline [HBS], pH 7.4) and brought to a final volume of 40 μL with HBS. The DBCO-NHS ester labeling reaction was incubated at room tempera-

ture for 30 min. DBCO-NHS ester labeling of the anti-human CD41 was then quenched by the addition of 2.5 μL of TRIS-HCl (1 M, pH 8.0). After quenching, 4.5 μL of ThS-P (2 mM, 10% DMSO by volume in HBS) was added to a final reaction volume of 47 μL . The ThS-P labeling reaction was incubated in the dark at room temperature for 4 h. ThS-Ab was isolated by gel filtration on P6-Gel maintained in HBS, resulting in 110 μL of purified ThS-Ab (0.05 mg mL^{-1} , as measured by absorption at 280 and Bradford assays) in HBS (Fig. 1). ThS-P and ThS-Ab fluorescence was measured in a FluoroSkan Ascent (485 nm excitation per 538 nm emission). ThS-Ab fluorescence on platelets was measured by flow cytometry (Accuri C6) based on a forward scatter/side scatter gate or by a positive signal for PE-anti-CD42b.

Microfluidic device for clotting on collagen/tissue factor surfaces

Polydimethylsiloxane (PDMS) microfluidic channels (250- μm wide \times 60 μm -high) were generated as previously described [8,18]. Tissue factor liposomes (PS/PC/bPE) were generated for linking to collagen via streptavidin-conjugated anti-collagen antibody [8,18,19]. A PDMS device was used to pattern fibrillar collagen (Chronolog, Havertown, PA, USA) in a 250- μm wide stripe followed by binding of the biotinylated lipidated TF. A second PDMS device created flow channels to run perpendicular across the collagen/TF surface. Whole blood with ThS-Ab (5 $\mu\text{g mL}^{-1}$) and Cy5-anti-fibrin (0.5 $\mu\text{g mL}^{-1}$) was perfused at a shear rate of 100 s^{-1} over the coated surface using a syringe pump (Harvard Apparatus PHD 2000, Holliston, MA, USA). Fluorescent microscopy (IX81; Olympus America Inc., Center Valley, PA, USA) was used to image clot formation in real time.

Microfluidic device for generation of transthrombus pressure gradient

An additional PDMS microfluidic device was used to create a transthrombus pressure gradient across a thrombus as it forms on a porous collagen/TF liposome surface (Fig. S1). Pressure was measured upstream, downstream and at the exit of the collagen scaffold using pressure transducers (Honeywell Sensing & Control, Golden Valley, MN, USA). The initial wall shear rate (521 s^{-1}) and constant pressure were maintained using an upstream syringe pump (Harvard Apparatus PHD Ultra, Holliston, MA, USA) containing CTI-treated whole blood along with a downstream syringe pump containing a Ca^{2+} buffer (5 mM). Each syringe pump was controlled by LabVIEW (National Instruments, Austin, TX, USA) to achieve a specified blood flow rate and pressure at the site of the collagen plug. Thrombotic events were visualized on a side view of the collagen scaffold which contained 50- μm -diameter posts and a 250- μm -long blood contact region [20,21]. Prior to loading the collagen scaffold onto the posts, the PDMS device was placed on a Sigmacote (Sigma-Aldrich)-treated glass slide and coated with 10% BSA for 30 min. Human type I collagen

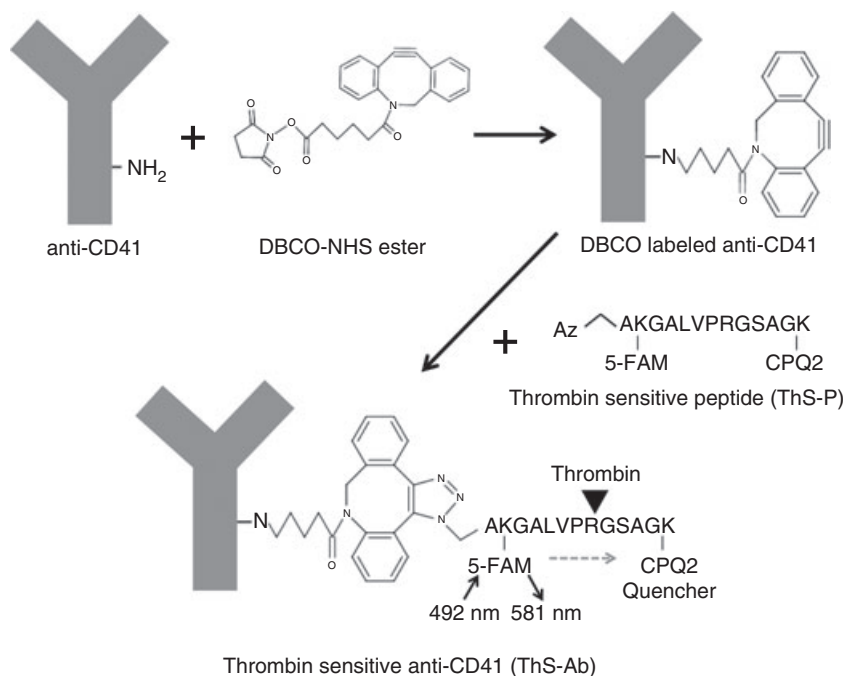


Fig. 1. Click chemistry for cross-linking a thrombin-sensitive N-terminal azidopeptide (ThS-P) to anti-CD41. Dibenzylcyclooctyne-NHS ester (DBCO) was used to label-free amine groups on anti-human CD41. The ThS-P contains a 5-FAM labeled Lys₂ and a CPQ2 (quencher) Lys₁₃. The Lys₂ and Lys₁₃ are separated by a thrombin cleavage site at Arg₈. The azide group specifically attacks the triple bond in DBCO linking the ThS-P to the anti-human CD41. Thrombin-mediated cleavage of the peptide releases the CPQ2 quencher, resulting in a fluorogenic signal at 581 nm.

(Advanced BioMatrix, San Diego, CA, USA) was polymerized at 2.4 mg mL⁻¹ in a ratio of 8:1:1 mixture of collagen, 0.09 M NaOH, 10× PBS. Biotinylated goat polyclonal anticollagen (4 μg mL⁻¹) and streptavidin (10 μg mL⁻¹) were subsequently added in 5-min intervals at a 1:10 ratio with polymerized collagen. TF liposomes were then added in a 1:20 ratio with collagen for 10 min. The collagen/TF solution was pulled through the upstream and downstream pressure ports into the collagen scaffold region on the device using a 1-mL syringe. Immediately after collagen/TF localization, the channels were rinsed with Ca²⁺ buffer (5 mM). Imaging protocols were identical to the previously mentioned device and real-time pressure data were collected through LabVIEW (Fig. S1B).

Mouse intravital microscopy

Mouse studies were approved by the IACUC of the University of Pennsylvania. Intravital microscopy was performed as previously described [22]. Mice were anesthetized with sodium pentobarbital (90 mg kg⁻¹), and maintained at 5 mg kg⁻¹ through a jugular vein cannula. The cremaster muscle was exposed and kept under a constant drip of buffer (135 mM NaCl, 4.7 mM KCl, 2.7 mM CaCl₂, 18 mM NaHCO₃, pH 7.4). The mThS-Ab (4.5 μg) and anti-mouse fibrin (5 μg) were infused into the mouse. Injuries, in selected arterioles, were made with a pulsed nitrogen dye laser at 440 nm. Confocal fluorescent and brightfield images were taken every 30 s for 10 min after injury using an Olympus BX-61WI fluorescence microscope (Olympus) coupled to a CSU-X1 spinning disk confocal head

(Yokogawa, Sugar Land, TX, USA) and CoolSnap HQ CCD camera (Photometrics, Tucson, AZ, USA).

Results

Characterization of thrombin cleavage of ThS-P and ThS-Ab

The Michaelis–Menten parameters for thrombin cleavage of ThS-P at 50 nM thrombin at 37 °C were $K_m = 40.3 \mu\text{M}$ and $k_{cat} = 1.5 \text{ s}^{-1}$ (Fig. 2A). The ThS-P signal in response to thrombin generated by whole blood activation was tested by addition of 0, 2.5 or 25 pM TF to citrated whole blood diluted 1:10 with HBS with 15 mM CaCl₂ (Fig. 2B). Without TF, the contact pathway was insufficient at this dilution of blood to generate ample thrombin during a 1600-s incubation (Fig. 2B, triangles). Upon the addition of increasing amounts of lipidated TF, the extrinsic tenase pathway was sufficient to trigger thrombin generation after a short initiation phase. The dose response and rates of thrombin cleavage of ThS-Ab were quite similar to those observed with ThS-P, indicating that the synthesis reaction did not significantly alter the kinetics of ThS-P cleavage by thrombin (Fig. 2C). To determine the specificity of thrombin cleavage of ThS-P, hirudin (1.75 μM), a thrombin specific inhibitor, was added to whole blood (treated with CTI and diluted 1:5 with Hepes buffer pH 7.4) in the presence of TF (25 pM) leading to complete ablation of ThS-P signal (Fig. S2), demonstrating that the sensor was highly specific for the detection of thrombin activity. The maximal ThS-Ab signal was approximately 50-fold less than that of the maximal ThS-P

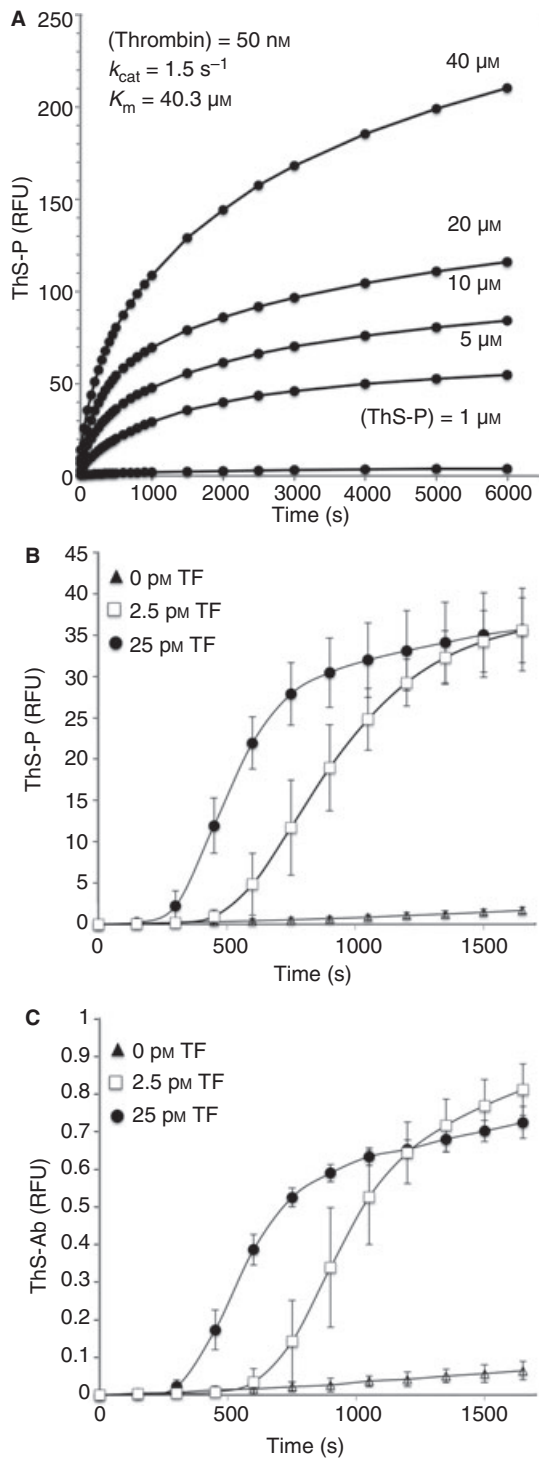


Fig. 2. Kinetics of ThS-P cleavage by thrombin was determined by titrating the ThS-P concentration in the presence of 50 nM thrombin. Thrombin cleavage resulted in a 35-fold increase in ThS-P fluorescence ($K_m = 40.3 \text{ } \mu\text{M}$ and $k_{cat} = 1.5 \text{ s}^{-1}$) (A). To determine if the synthesis of ThS-Ab affected the rate of cleavage by thrombin both ThS-Ab (0.05 mg mL^{-1}) (B) and ThS-P ($5 \text{ } \mu\text{M}$) (C) were added to citrated whole blood (re-calcified) with added tissue factor (TF 2.5 or 25 pM). Both ThS-P and ThS-Ab had similar rates of cleavage as well as a dose response to increasing amounts of TF.

signal owing to the concentration of the ThS-Ab stock solution ($50 \text{ } \mu\text{g mL}^{-1}$) deployed in order to avoid over-diluting the blood.

Platelet surface localization of ThS-Ab and signal in response to thrombin

To detect thrombin activity on the platelet surface, flow cytometry was performed on whole blood labeled with ThS-Ab in the presence or absence of added TF (25 pM ; Fig. 3). Citrated whole blood was incubated for 5 min with ThS-Ab ($10 \text{ } \mu\text{g mL}^{-1}$) and then diluted 1:10 with the addition of 5 mM GPRP peptide to prevent fibrin polymerization and 15 mM CaCl_2 . Without the addition of TF, very little change in the ThS-Ab signal was observed after 15 min (Fig. 3A). With 25 pM TF, thrombin was generated as indicated by a 20-fold increase in signal by 14 min. To confirm the ThS-Ab signal was platelet specific, only cells positive for CD42b were positive for the ThS-Ab signal in response to thrombin generation (Fig. S3).

Thrombin sensing in a microfluidic model of thrombosis

Thrombin localization within a growing thrombus under hemodynamic conditions was observed by perfusion of ThS-Ab labeled whole blood (CTI-treated) over a patterned collagen surface with antibody-linked lipidated TF at a shear rate of 100 s^{-1} . The collagen patterning of a stripe resulted in a discrete $250 \text{ } \mu\text{m}$ wide \times $250 \text{ } \mu\text{m}$ long square of collagen when the fluidic channel was overlaid perpendicular to the stripe. The upstream end of this discrete collagen region can be seen in Figs 4 and S3. At 0, 0.1 or 1 molecule-TF μm^{-2} (as determined based on ref. [18]), the simultaneous platelet deposition, fibrin deposition and ThS-Ab signal were monitored in real time (Fig. 4A–C). Whole blood with the thrombin inhibitor PPACK ($100 \text{ } \mu\text{M}$) was perfused over the 1 molecule-TF μm^{-2} surface. In comparing Fig. 4C and 4D where blood was perfused over TF-labeled collagen with and without PPACK, PPACK caused a $> 50\%$ decrease in platelet deposition and blocked the detectable fibrin signal. However, even $100 \text{ } \mu\text{M}$ PPACK was unable to fully block generation of the ThS-Ab signal (Fig. 4D). This indicated that thrombin produced as a result of the TF surface was able to cleave the platelet bound ThS-Ab before cleaving fibrinogen or encountering PPACK. Thus, ThS-Ab was a more sensitive metric of local thrombin production than antibody-based detection of fibrin polymerization.

At 0.1 molecule-TF μm^{-2} , the amount of thrombin generation decreased by approximately 65% (as indicated by fluorescence intensity) compared with 1 molecule-TF μm^{-2} . Unique localized zones of thrombin generation were detectable at early times during thrombus formation (especially near the side walls of the device) that coexisted with other zones in the image field that lacked ThS-Ab fluorescence (Fig. S3). During early time points of blood perfusion over 0.1 molecule-TF μm^{-2} , slightly more platelet deposition was seen at

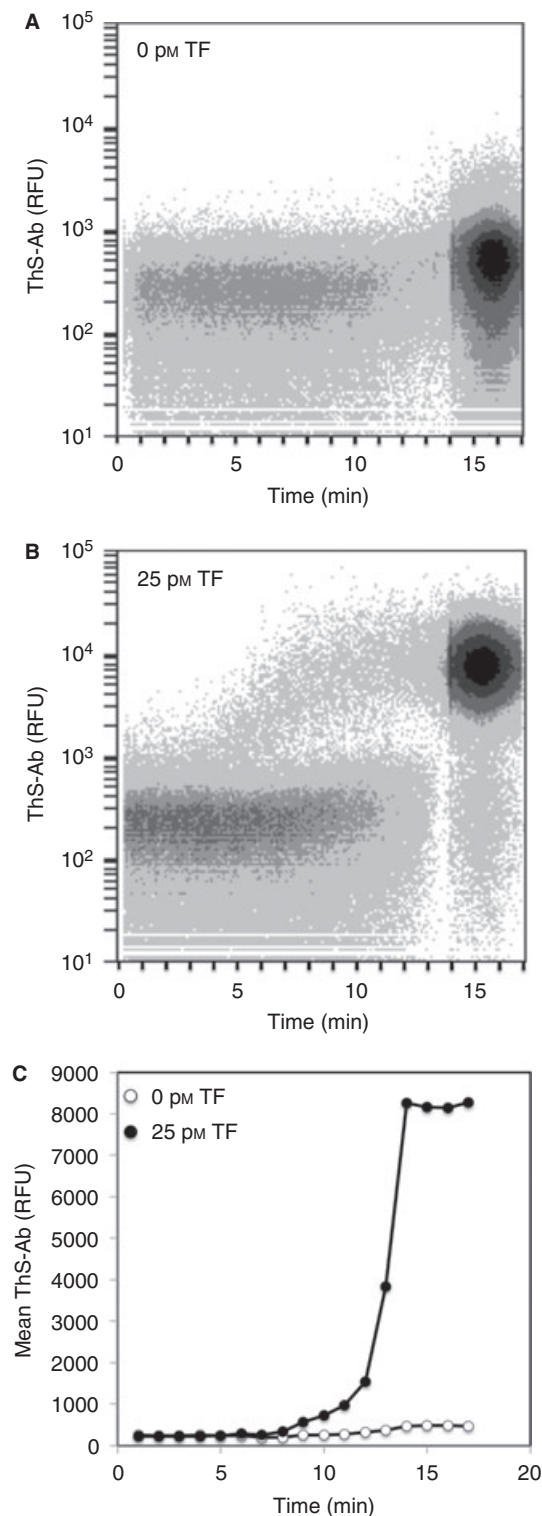


Fig. 3. Real-time flow cytometry of whole blood labeled with ThS-Ab to detect platelet localized thrombin activity after the addition of tissue factor (TF). Whole blood was incubated with ThS-Ab (1:50 volume) either in the absence (A) or presence of 25 pM TF (B). The mean fluorescence of the gated events demonstrated that TF caused a large increase in the platelet-specific thrombin signal (C).

the front of the collagen/TF surface whereas the ThS-Ab and anti-fibrin signal was located down stream of the platelet mass (as previously observed in ref. [8]). This indicated that the observed signal was in fact owing to increased levels of thrombin activity and not increased platelets with bound ThS-Ab. The shear rates on the periphery side walls of the flow chamber were lower than in the center with consequent reduced rates of dilution of thrombin from the surface into the flow stream, thus allowing for increased accumulation of thrombin and fibrin along the periphery of the chamber [23]. Without added TF, no thrombin or fibrin was formed after 450 s. After 10–13 min of flow over collagen (no TF), ThS-Ab fluorescence and fibrin formation were finally detected (not shown), most probably owing to formation of XIIa in spite of the presence of CTI [10].

Microfluidic model of transthrombus pressure gradient-driven permeation during hemostasis

As a thrombus builds up at a site of vascular rupture or wounding, a pressure drop (ΔP) exists across the clot because the intraluminal pressure (up to arterial levels of 60–120 mm Hg) exceeds the interstitial pressure (approximately 10–12 mm Hg) [24,25]. The pressure-driven permeation of plasma or serum across the porous clot structure and into the porous interstitial matrix at the point of injury represents a convective transport mechanism. To drive transthrombus permeation, a microfluidic device was developed that allowed a thrombus to form on a supported porous collagen plug at a controlled shear rate of blood perfusion (Fig. 5A). As the atmospheric pressure was maintained on the opposite (non-blood contacting) side of the collagen plug, a controlled pressure drop independent of the wall shear rate was maintained across the collagen and thrombus (Figs 5A and S1), thus mimicking a bleed into the interstitial space. The pressure drop was set to $\Delta P = 3200$ Pa (32 mm Hg) or $\Delta P = 0$ Pa (by blocking the outlet) to control the permeating flow across the thrombus (Fig. S1). Blood labeled with ThS-Ab, fluorescent anti-CD61 and fluorescent anti-fibrin was perfused at 521 s^{-1} over the collagen/TF plug. At $\Delta P = 3200$ Pa, the increased permeation of thrombin across the thrombus resulted in the ThS-Ab signal being only present in thin areas within the thrombus nearest the collagen/TF surface (Fig. 5B). At $\Delta P = 3200$ Pa, ample fibrin was formed within the collagen owing to permeation of thrombin and fibrinogen into the collagen (Fig. 5D). Without a pressure drop ($\Delta P = 0$), the thrombin transport within the thrombus was largely because of diffusion as no permeation across the collagen was possible. This resulted in a five-fold increase in the ThS-Ab signal generated within the thrombus, compared with the case of $\Delta P = 3200$ Pa (Fig. 5B,C). The fibrin signal was measured at the surface of the collagen/TF matrix as well as $10 \mu\text{m}$ into the thrombus to observe the rate of deposition (Fig. S5). At the surface of the collagen/TF matrix, the rate of fibrin deposition was unchanged by the change in ΔP and altered thrombin localization pattern (Fig. S5A). However, at

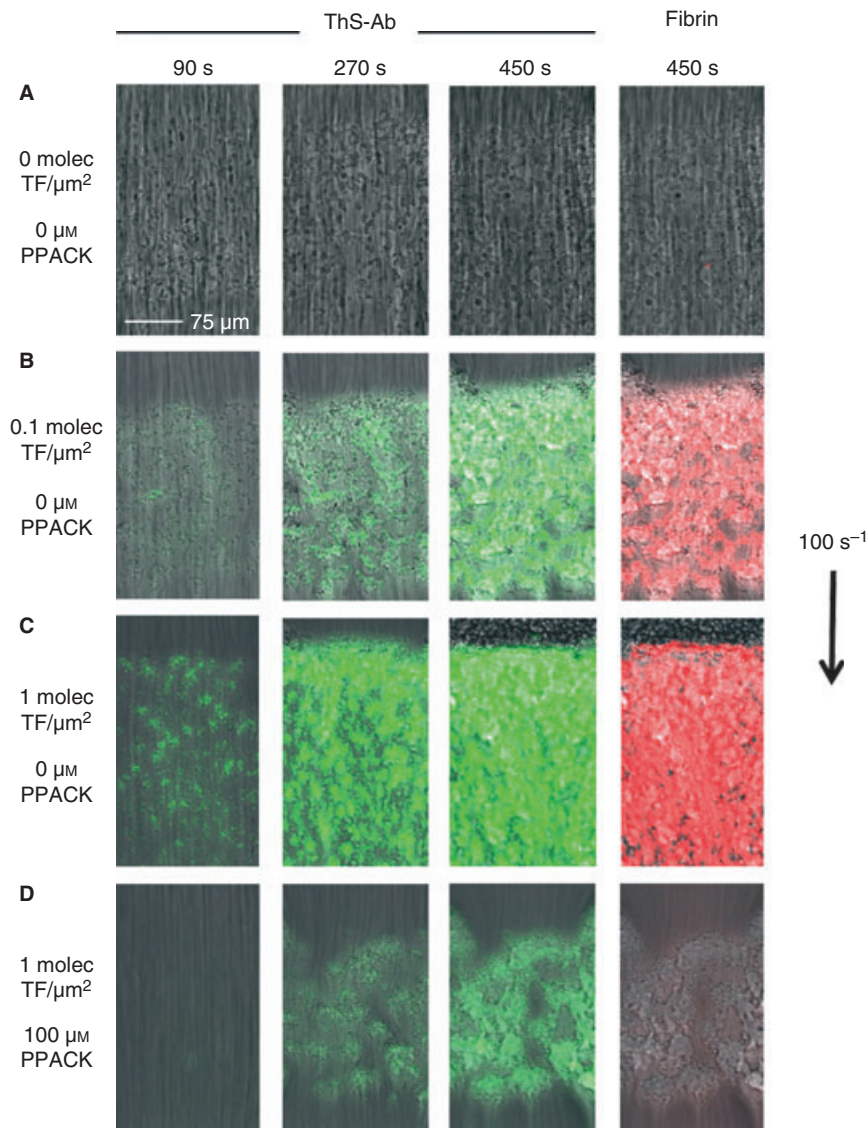


Fig. 4. Detection of thrombin in a blood clot forming under flow conditions. A microfluidic model of coagulation was generated by flowing whole blood (100 s^{-1}) over collagen with linked lipidated tissue factor (TF). ThS-Ab (green) and fibrin (red) were observed over time whereas flowing over collagen (A), collagen and TF ($0.1 \text{ molecule } \mu\text{m}^{-2}$) (B), collagen and TF ($1 \text{ molecules } \mu\text{m}^{-2}$) alone (C), and collagen and TF ($1 \text{ molecules } \mu\text{m}^{-2}$) in the presence of $100 \text{ } \mu\text{M}$ PPACK (D).

$10 \text{ } \mu\text{m}$ into the thrombus, the rate of fibrin deposition was decreased approximately 45% when $\Delta P = 3200 \text{ Pa}$ and thrombin levels were decreased within the thrombus (Fig. S5B).

In vivo monitoring of thrombin within a thrombus

Laser-induced injury created stable thrombi in mouse cremaster arterioles [22]. Mice were perfused with anti-fibrin and ThS-Ab anti-mouse CD41 (mThS-Ab) prior to injury. Images were taken of the bright field thrombus formation as well as fibrin deposition and mThS-Ab every 30 s for 10 min. Similar to microfluidic model thrombosis, the mouse thrombi showed a core of mThS-Ab signal that co-localized with fibrin deposition (Fig. 6 and Movie S1). Thrombus growth was stabilized where

the high mThS-Ab signal was present, as low mThS-Ab regions appeared to be more prone to shearing forces of the blood flow and disassociated from the thrombus over time. The stable thrombus core nearest the injury site had the highest mThS-Ab signal and was anchored by a layer of fibrin deposition at the vessel wall at the site of injury. During early thrombosis, the thrombus mass was large with a core of a high mThS-Ab signal and a more diffuse signal occurred in the outer zones of the thrombus. After 5 min, the remaining clot was stable and had a high mThS-Ab signal and high fibrin deposition (Fig. 6). To specifically inhibit thrombin function, $15 \text{ } \mu\text{g}$ of hirudin was infused prior to injury and inhibited $> 90\%$ of the ThS-Ab signal 2 min post-injury (Fig. S6). Similar to the *in vitro* findings with hirudin, ThS-Ab is a specific detector of thrombin activity, even in an *in vivo* thrombotic setting.

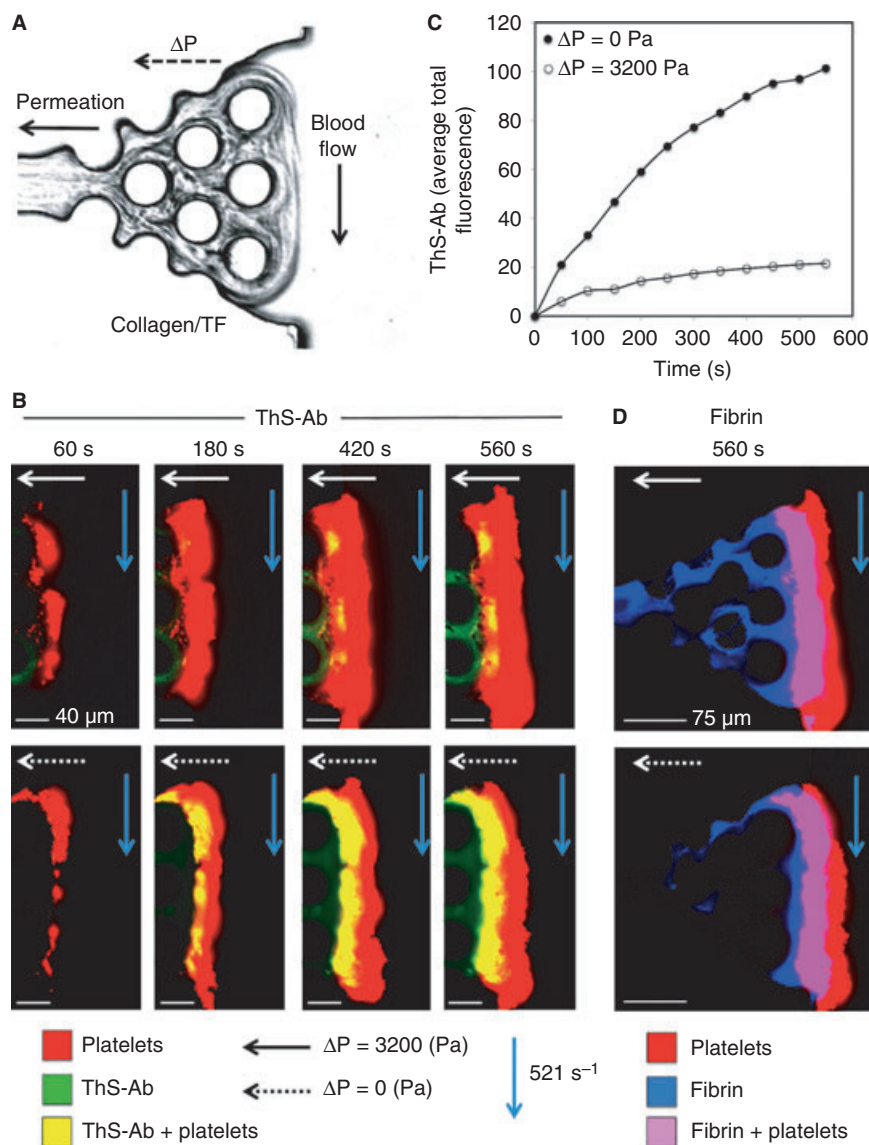


Fig. 5. A thrombogenic surface of collagen and TF was used in a microfluidic device to provide a side view of thrombus formed under flow conditions whereas a transthrombus pressure gradient drives permeation across the clot (A). Blood was perfused at 521 s^{-1} and ThS-AB (green), anti-fibrin (blue) and anti-CD61 (red) were observed over time during thrombus formation. The pressure drop across the surface was altered to change the transport pattern of thrombin ($\Delta P = 3200$ or 0 Pa) (B). The pressure drop caused a decrease in thrombin presence in the clot (C). To quantify the rate of fibrin deposition, the fluorescence signal of anti-fibrin was monitored at different distances from the coagulation surface (0 and $10 \mu\text{m}$) for the different pressure drop states (D).

Discussion

The localization of thrombin is dictated by the site of generation and the movement of thrombin which is controlled by diffusion, binding and convection. Detection of thrombin activity via fluorogenic substrates is less suited under flow conditions owing to convective removal of the soluble reporter. In this study, we report, for the first time, detection of intrathrombus thrombin activity under flow conditions using ThS-Ab in microfluidic assays and in mouse.

In order for ThS-Ab to serve as a stable marker for platelet surface-thrombin activity, it must localize to the surface of platelets and provide a robust signal upon thrombin genera-

tion. Using flow cytometry, platelets displayed an approximately 20-fold increase of the ThS-Ab signal after 10 min of incubation with TF (Fig. 3). Platelets became positive for the ThS-Ab signal, as determined by co-staining with platelet-specific anti-CD42b and the ThS-Ab signal (Fig. S3). ThS-P cleavage has a $k_{\text{cat}}/K_m = 0.375$ whereas fibrinogen has a $k_{\text{cat}}/K_m = 11.3$ [26]. In spite of the difference in kinetics, both *in vitro* and *in vivo* thrombosis models showed fibrin deposition and the ThS-Ab signal as spatially and temporally co-localized (Figs S4 and 6).

To visualize the activity of thrombin within a hemostatic thrombus, a microfluidic device was used to trigger thrombosis on a pro-coagulant surface (collagen and TF) which provided a

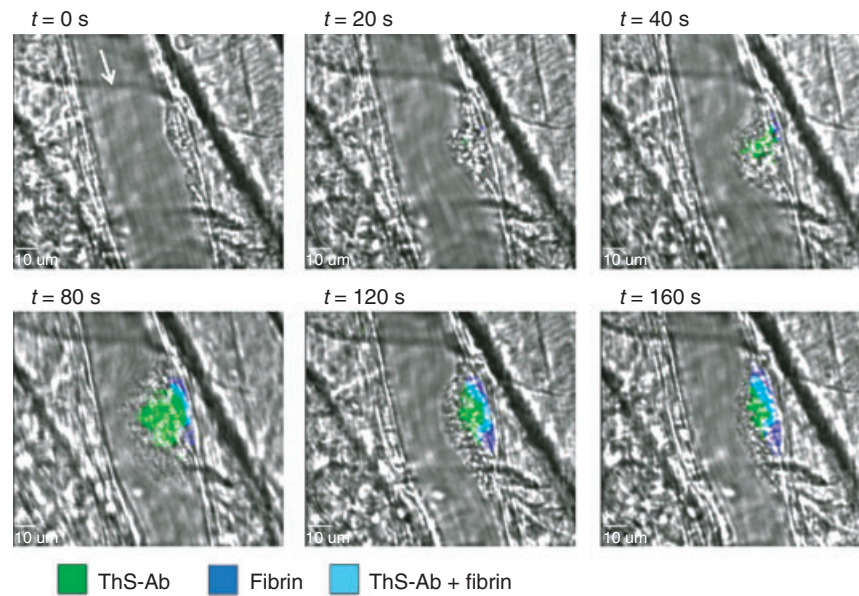


Fig. 6. A mouse laser injury model was used to observe the mThS-Ab signal *in vivo*. A mouse laser injury model was used to observe the mThS-Ab signal *in vivo*. The site of injury was observed using confocal fluorescent microscopy. Blood flow is denoted by an arrow at $t = 0$ s. The ThS-Ab signal (green) is first observed at 40 s post-injury that co-localizes with fibrin (blue). As the clot grows, the ThS-Ab signal spreads away from the vessel wall as fibrin stays close to the vessel wall. After 2 min post-injury, the clot begins shrinking and the core remains the area of high fibrin and a high ThS-Ab signal and a shell of platelets that are thrombin negative.

side-view observation. To further enhance the physiological relevance of this microfluidic system, a pressure drop was established across the pro-coagulant surface to study the effect of transthrombus permeation (Fig. 5A). We have demonstrated (Fig. S7) that there is plasma loss using fluorescent plasma tracers as well as visible red blood cell escape into the endothelial space after laser injury. The microfluidic device in Fig. 5 recreates certain aspects of *in vivo* vessel injury such as movement of blood or plasma across a porous clot or wall structure owing to a pressure-driven permeation or flow. By combination of ThS-Ab with a novel microfluidic device that mimics hemostasis, this is the first study of thrombin levels in clots formed with a transthrombus pressure drop to drive permeation in a direction perpendicular to blood flow and in the direction of the interstitial space. Transthrombus permeation into the interstitial space reduced platelet-associated thrombin activity and enhanced fibrin polymerization into the interstitial region (Fig. 5B,D). Fibrin is shown to occur in the interstitial space especially when a pressure drop exists across the collagen-TF/thrombus surface (Figs 5D and S8). With a zero pressure drop, the high level of thrombin formed at the collagen-TF/platelet interface (Fig. 5B) resulted in rapid fibrinogen conversion to immobile fibrin, which does not move into the collagen region. When the pressure drop is present, lower levels of thrombin accumulate (possibly because of dilution by permeation into the interstitial space). Fibrinogen and lower levels of fibrin monomer can thus undergo permeation into the collagen region. This allows the fibrin to polymerize within the interstitial region as fibrin monomer is driven by the permeation of plasma through the interstitial

space. While fibrin polymers are unable to penetrate into the interstitial space, thrombin is still highly diffusible and can enter into the interstitial space even without pressure drop induced flow. ThS-Ab free in solution is also able to penetrate into the interstitial area by diffusion. Consistent with the *in vitro* observation of Fig. 5, interstitial fibrin has routinely been detected in the mouse laser injury model (T.J.S., data not shown). While not well studied, the formation of fibrin in the interstitial region outside a blood vessel may be an attribute of *in vivo* hemostasis owing to pressure driven-permeation across a platelet mass.

To verify the ThS-Ab sensor in an *in vivo* context, ThS-P was attached to anti-mouse CD41, infused into mice and observed after laser injury of the cremaster muscle (Fig. 6). Platelets quickly formed a plug at the site of injury without thrombin activity ($t = 0$ s), and 20 s after the injury both the fibrin and thrombin signal appeared at the site of injury (Fig. 6 and Movie S1). The fibrin signal was localized close to the vessel wall whereas the thrombin signal was highest close to the vessel wall but thrombin appeared to diffuse out into the thrombus as well. After 80 s post-injury, there was a large amount of fibrin deposition along the vessel wall that co-localized with the highest concentration of thrombin activity; however, lower thrombin activity was also detected away from the vessel wall in the thrombus, but thrombin activity was not detected in the outer most shell of the thrombus. After 80 s post-injury, the thrombus decreased in size and the area positive for the platelet also decreased, as the outer most shell of the thrombus remained thrombin negative. These results indicate that thrombin initially localizes at high concentrations at the site of injury and was

capable of producing fibrin. Decreased thrombin activity and increased convection may also contribute to the lack of fibrin formation further away from the vessel wall. At 160 s post-injury, the fibrin plug and areas of high thrombin activity remain stable with an outer shell of thrombin-negative platelets. These results show that thrombin was produced at the site of injury and was most active along the vessel wall leading to a stable fibrin plug. Thrombin was also active further from the vessel wall but to a lesser extent and did not produce stable platelet deposits or fibrin polymers at large distances from the site of injury (Fig. 6). To our knowledge, this is the first direct imaging of thrombin activity in a forming thrombus *in vivo*.

The use of a fluorogenic peptide sequence linked to an antibody by click chemistry represents a simple and general approach for visualizing proteases. The approach may have also utility for the study of other proteases involved in thrombosis, inflammation or metastasis. We demonstrated that thrombin activity can be detected on the time frame of a real clotting event. The sensor allowed a very sensitive detection of thrombin in situations where fibrin was not necessarily generated. Also local transport processes within the clots were shown to modulate the thrombin signal.

Disclosure of Conflict of Interest

The authors state that they have no conflict of interest.

Supporting Information

Additional Supporting Information may be found in the online version of this article:

Figure S1. A microfluidic device for perfusion of blood at flow rate Q1 from an inlet across a collagen plug that covers an outlet maintained at P3 = atmospheric pressure.

Figure S2. The cleavage of ThS-P was monitored using a fluorescent plate reader.

Figure S3. Flow cytometry of clotting whole blood demonstrated that the ThS-Ab signal detected thrombin generation specifically on platelet surfaces.

Figure S4. During platelet deposition on collagen/TF surfaces, the platelet deposits displayed heterogeneity in thrombin activity and fibrin deposition.

Figure S5. Fibrin deposition at the collagen/thrombus surface (0 μm) or 10 μm depth into the thrombus was measured using anti-fibrin fluorescence after 560 s of whole blood flow (521 s^{-1}) (A). The rate of fibrin deposition at the collagen/thrombus surface was quantified and appeared largely unaffected by the presence or absence of a pressure drop across the fibrin (B). The rate of deposition fibrin deposition at 10 μm into the thrombus was significantly reduced by the presence of a pressure drop across the thrombus (3200 Pa) (C).

Figure S6. Intravital microscopy of the mouse laser injury model was used to monitor the ThS-Ab and fibrin signal during thrombosis.

Figure S7. Intravital microscopy of the mouse laser injury model acquired immediately after injury.

Figure S8. In (A), fibrin is shown occurring in the interstitial space especially when a pressure drop exists across the collagen-TF/thrombus surface. With a zero pressure drop, the high level of thrombin formed at the collagen-TF/platelet interface (B) resulted in rapid fibrinogen conversion to immobile fibrin which does not move into the collagen region. When the pressure drop is present, lower levels of thrombin accumulate (possibly because of dilution by permeation into the interstitial space). Fibrinogen and lower levels of fibrin monomer can thus undergo permeation into the collagen region. This allows the fibrin to polymerize within the interstitial region as the fibrin monomer is driven by the permeation of plasma through the interstitial space. In contrast, without the pressure drop, the fibrin polymers are unable to penetrate deeply into the interstitial space, as there is a lack of flow across the surface. While fibrin polymers are unable to penetrate into the interstitial space, thrombin is still highly diffusible and can enter into the interstitial space even without pressure drop induced flow. ThS-Ab free in solution is also able to penetrate into the interstitial area by diffusion, therefore, the presence of a pressure drop that induces flow across the interstitial space and to the outlet can lead to wash out of the thrombin and ThS-Ab. Thus in (B) the ThS-Ab signal observed without a pressure drop is the accumulation of the cleaved ThS-Ab during the experiment. While the ThS-Ab signal with the pressure drop is subject to continuous wash out thus leading to signals that cannot be accurately compared with quantify interstitial thrombin activity, which is platelet-linked.

Movie S1. Intravital microscopy of the mouse laser-injury model was used to monitor ThS-Ab fluorescence during injury-induced thrombosis (as previously described).

Please note: Wiley-Blackwell is not responsible for the content or functionality of any supporting materials supplied by the authors. Any queries (other than missing material) should be directed to the corresponding author for the article.

References

- Leiderman K, Fogelson AL. Grow with the flow: a spatial-temporal model of platelet deposition and blood coagulation under flow. *Math Med Biol* 2011; **28**: 47–84.
- Diamond SL. Engineering design of optimal strategies for blood clot dissolution. *Annu Rev Biomed Eng* 1999; **1**: 427–62.
- Okorie UM, Denney WS, Chatterjee MS, Neeves KB, Diamond SL. Determination of surface tissue factor thresholds that trigger coagulation at venous and arterial shear rates: amplification of 100 fM circulating tissue factor requires flow. *Blood* 2008; **111**: 3507–13.
- Kuharsky AL, Fogelson AL. Surface-mediated control of blood coagulation: the role of binding site densities and platelet deposition. *Biophys J* 2001; **3**: 1050–74.
- Dormann D, Clemetson KJ, Kehrel BE. The GPIb thrombin-binding site is essential for thrombin-induced platelet procoagulant activity. *Blood* 2000; **96**: 2469–78.
- Celikel R, McClintock RA, Roberts JR, Mendolicchio GL, Ware J, Varughese KI, Ruggeri ZM. Modulation of α -thrombin function by

- distinct interactions with platelet glycoprotein Iba. *Science* 2003; **301**: 218–21.
- 7 Hathcock JJ, Nemerson Y. Platelet deposition inhibits tissue factor activity: in vitro clots are impermeable to factor Xa. *Blood* 2004; **1**: 123–7.
 - 8 Colace TV, Muthard R, Diamond SL. Thrombus growth and embolism on tissue factor bearing collagen surfaces under flow: role of thrombin with and without fibrin. *Arterioscler Thromb Vasc Biol* 2012; **32**: 1466–76.
 - 9 Gailani D, Broze GJ Jr. Factor XI activation in a revised model of blood coagulation. *Science* 1991; **23**: 909–12.
 - 10 Esmon CT, Fukudome K, Mather T, Bode W, Regan LM, Stearns-Kurosawa DJ, Kurosawa S. Inflammation, sepsis and coagulation. *Haematologica* 1999; **84**: 254–9.
 - 11 Ito Y, Liu LS, Imanishi Y. Interaction of thrombin with synthetic fluorescent substrate immobilized on polymer membrane. *Biomaterials* 1992; **13**: 375–81.
 - 12 Cho H, Baker BR, Wachsmann-Hogiu S, Pagba CV, Laurence TA, Lane SM, Lee LP, Tok JBH. Aptamer-based SERRS sensor for thrombin detection. *Nano Lett* 2008; **8**: 4386–90.
 - 13 Handin RI, Lux SE, Stossel TP. *Blood: Principles and Practice of Hematology*. Philadelphia, PA: Lippincot Williams and Wilkins, 2003; 1168 pp.
 - 14 Chatterjee MS, Denney WS, Jing H, Diamond SL. Systems biology of coagulation initiation; kinetics of thrombin generation in resting and activated human blood. *PLoS Comput Biol* 2010; **9**: e1000950.
 - 15 Hemker HC, Giesen P, Al Dieri A, Regnault V, de Smedt E, Wagenvoort R, Lecompte T, Beguin S. Calibrated automated thrombin generation measurement in clotting plasma. *Pathophysiol Haemost Thromb* 2003; **33**: 4–15.
 - 16 Guy RD, Fogelson AL, Keener JP. Fibrin gel formation in a shear flow. *Math Med Biol* 2007; **1**: 111–30.
 - 17 Neeves KB, Illing DA, Diamond SL. Thrombin flux and wall shear rate regulate fibrin fiber deposition state during polymerization under flow. *Biophys J* 2010; **7**: 1344–52.
 - 18 Colace TV, Jobson J, Diamond SL. Relipidated tissue factor linked to collagen surfaces potentiates platelet adhesion and fibrin formation in a microfluidic model of vessel injury. *Bioconjug Chem* 2011; **22**: 2104–9.
 - 19 Smith SA, Morrissey JH. Rapid and efficient incorporation of tissue factor into liposomes. *J Thromb Haemost* 2004; **2**: 1155–62.
 - 20 Sudo R, Chung S, Zervantonakis IK, Vickerman V, Toshimitsu Y, Griffith LG, Kamm RD. Transport-mediated angiogenesis in 3D epithelial coculture. *FASEB J* 2009; **7**: 2155–64.
 - 21 Polacheck WJ, Charest JL, Kamm RD. Interstitial flow influences direction of tumor cell migration through competing mechanisms. *Proc Natl Acad Sci USA* 2011; **27**: 11115–20.
 - 22 Stalker TJ, Wu J, Morgans A, Traxler EA, Wang L, Chatterjee MS, Lee D, Quertermous T, Hall RA, Hammer DA, Diamond SL, Brass LF. Endothelial cell specific adhesion molecule (ESAM) localizes to platelet-platelet contacts and regulates thrombus formation in vivo. *J Thromb Haemost* 2009; **11**: 1886–96.
 - 23 Neeves KB, Maloney SF, Fong KP, Schmaier AA, Kahn ML, Brass LF, Diamond SL. Microfluidic focal thrombosis model for measuring murine platelet deposition and stability: PAR4 signaling enhances shear-resistance of platelet aggregates. *J Thromb Haemost* 2008; **6**: 2193–201.
 - 24 Wiig H. Evaluation of methodologies for measurement of interstitial fluid pressure (Pi): physiological implications of recent Pi data. *Crit Rev Biomed Eng* 1990; **18**: 27–54.
 - 25 Parzynski SE, Hargens AR, Tucker B, Aratow M, Styf J, Crenshaw A. Transcapillary fluid shifts in tissues of the head and neck during and after simulated microgravity. *J Appl Physiol* 1991; **71**: 2469–75.
 - 26 Higgins DL, Lewis SD, Shafer JA. Steady state kinetic parameters for the thrombin-catalyzed conversion of human fibrinogen to fibrin. *J Biol Chem* 1983; **10**: 9276–82.